

NUMERICAL INVESTIGATION OF FLOW IN RADIAL DIFFUSERS WITH FEEDING ORIFICE MODIFIED

André Esperandio

Mechanical Engineering Undergraduate Program

William de Araújo Jacques

Mechanical Engineering Graduate Program – PPGEM

william.jacques@pucpr.br

Viviana Cocco Mariani

Mechanical Engineering Graduate Program – PPGEM

Pontifical Catholic University of Parana – PUCPR

80215-901 – Curitiba, PR, Brazil

viviana.mariani@pucpr.br

Abstract. *Radial diffusers are the basic geometry for the automatic valves in reciprocating hermetic compressors. The present work considers the numerical modeling of laminar flow in radial diffuser with axial feeding. The bi-dimensional governing equations are numerically solved using the finite volume methodology with mixed Eulerian Lagrangian method. The numerical model was able to handle irregular geometries making use of a regular mesh, and was validated through comparisons with experiments. The numerical results presented in this work are the dimensionless axial force acting on the valve disc and the dimensionless effective flow and force areas that are important efficiency parameters for the modelling and design of reciprocating hermetic compressors. The efficiency parameters are presented and explored in terms of different Reynolds numbers varying from 1000 to 2500 and three values of the gap between valve reed and valve seat. Numerical results of pressure distribution on the front disk surface for different flow conditions when compared to the experimental data indicated that with a small chamfer of 5° at the outlet of the valve feeding orifice, the efficiency parameters were improved for example, effective force and flow area were increased.*

Keywords: *radial diffuser, feeding orifice, seat inclination, Reynolds number*

1. INTRODUCTION

The geometry of automatic valves in hermetic compressors can be approximated by a radial diffuser and your geometric parameters as shown in Figs. 1a and 1b, respectively. In this geometry the fluid flows axially through a feeding orifice with diameter d , and then is deflected along the radial direction by the frontal disk, represented in the figure by the valve reed with diameter D . In the present investigation the flow is assumed laminar and axially symmetric.

Both suction and discharge valves in hermetic compressors function according to the existing pressure difference between the interior of the cylinder and the suction and discharge chambers, respectively, and the opening and closing forces resulted from the pressure difference are dictated by the piston reciprocating movement. Geometrically, among the main components that can be optimized in those valves are the dimensions and shape of the seat, feeding orifice and reed. Optimum valves operate at high efficiency which is evaluated by two parameters: effective flow and force areas. Those two parameters play an important role in modeling and designing of automatic valves.

The literature on radial flow is extensive and some representative contributions are due to Hayashi *et al.* (1975), Ervin *et al.* (1989) and Tabatabai and Pollard (1987). For radial flow in the context of compressor valves the reader is referred to Ferreira and Driessen (1986), Ferreira *et al.* (1989), Prata and Ferreira (1990), Prata *et al.* (1995), Deschamps *et al.* (2000) and Possamai *et al.* (2001).

Ferreira and Driessen (1986) presented a discussion of the flow patterns encountered in reed type valves and reviewed the literature up to then. A numerical and experimental solution for the laminar isocoric flow field of air in radial diffusers, for small separation between discs, was explored by Prata *et al.* (1995), Ferreira *et al.* (1989) and Possamai *et al.* (2001). More recently numerical and experimental resulted for the turbulent flow were presented by Deschamps *et al.* (2000). Following this line Salinas-Casanova (2001) and Matos (2002) presented a numerical and experimental solution for three dimensional turbulent flow field of air in radial diffusers, using the models $k-\epsilon$ and RNG $k-\epsilon$. Mariani (2002, 2006) investigated the modification the geometric parameters on radial diffuser solving laminar flow for different separation between discs and for various Reynolds numbers. Of the previous work on radial diffuser investigated only Puff *et al.* (1992) and Mariani (2002, 2006) studied the geometric parameter explored in the present work.

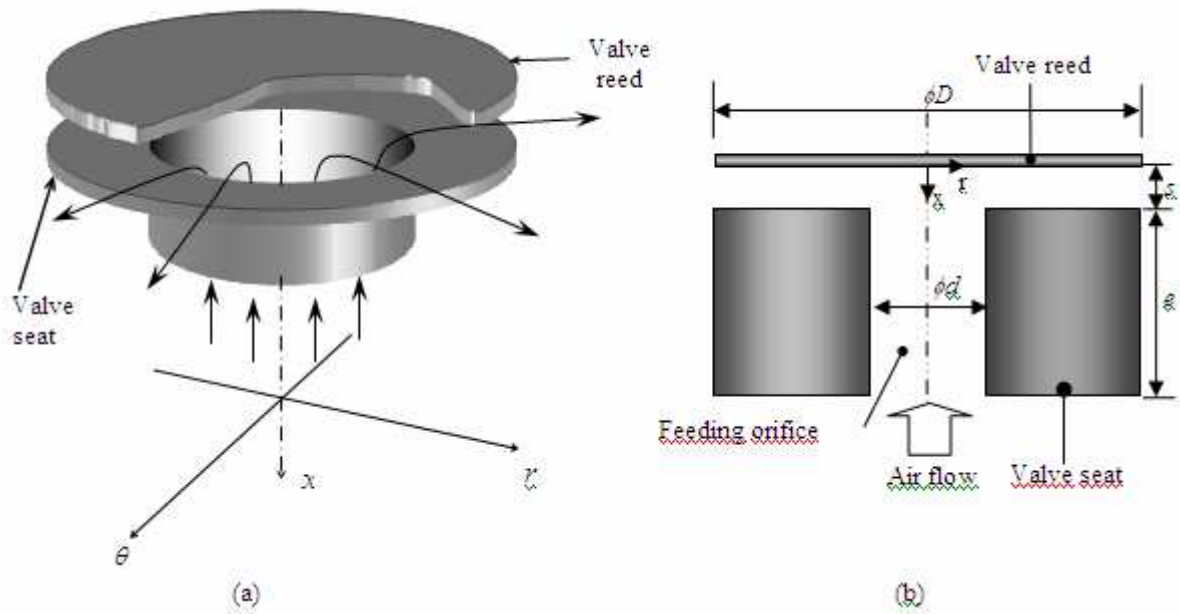


Figure 1. Geometry of radial diffuser with axial feeding, without chanfre in seat.

Valve geometry has a significant influence on the effective flow and force areas, and one of the purposes of the present work is to investigate the influence of geometric parameters such as seat inclination on the dimensionless effective flow and force areas. With this objective is presented the Figs. 2a and 2b, respectively, the geometry of automatic valves with a chanfre in seat and your approximation by a three dimensional radial diffuser and your geometric parameters.

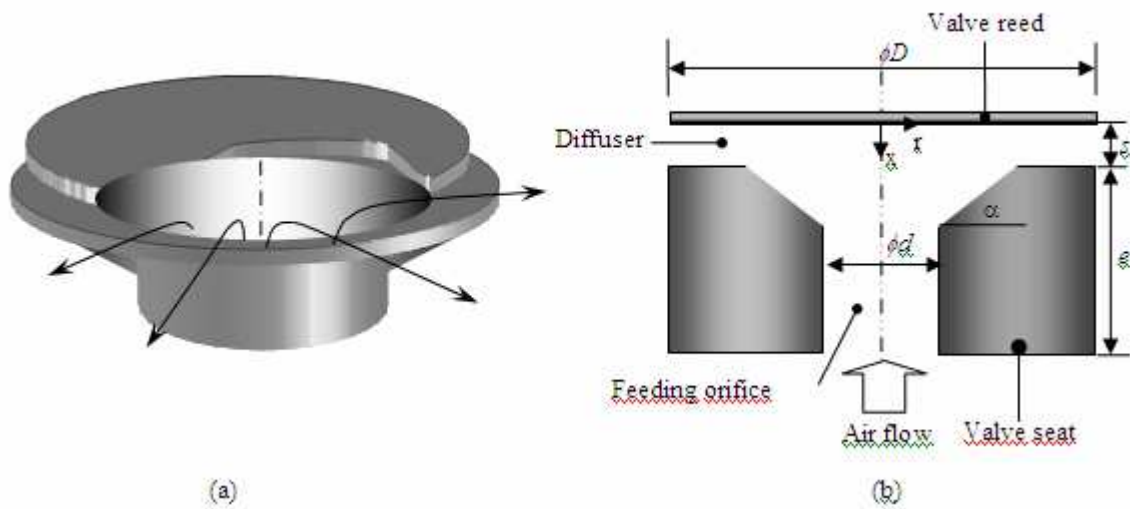


Figure 2. Geometry of radial diffuser with axial feeding and chanfre in seat.

The governing differential equations in cylindrical coordinates for the problem considered here are numerically integrated using the finite volume methodology. Because the solid surfaces for different shapes of the seat do not coincide with the cylindrical coordinates employed in the domain discretization, use was made of the *Eulerian Lagrangian Algorithm For INterface Tracking* (ELAFINT). The ELAFINT methodology (Udaykumar *et al.*, 1996; Ye *et al.*, 1999) shapes the volumes with irregular format that are in the interface between fluid and solid. With this methodology the control volumes are regular and proper for discretization in cylindrical coordinates within the flow passages, and at the flow boundaries the volumes become trapezoidal to accommodate for the solid walls.

This paper presents the results experimental and numerical exploring the pressure distribution on the valve reed as a function of the gap between the disks and the flow Reynolds number. In that follows, dimensionless effective flow and force areas for different magnitudes of seat inclination and different valve diameters, for various flow Reynolds number

and valve separations are presented. These results are calculated for laminar incompressible flow and for small distances between valve and seat.

The present work is organized according to the present form: next section explores the partial differential equations that model the flow field across the valve; section three validates the numerical solution and the ELAFINT methodology comparing dimensionless pressure profile obtained both numerically and experimentally; the numerical results presented in section four are pressure profiles on the valve disc, the dimensionless axial force acting on the valve disc and the dimensionless effective flow and force areas; and in the last section some conclusions are offered.

2. PROBLEM FORMULATION

The geometries of radial diffusers with modified parameters investigated in the present work are presented in Figure 2. As the flow is axially symmetric, only one angle is studied along the diffuser circumference, simulating a bi-dimensional problem. The basic assumptions employed in simplifying the problem are isothermal, isocoric, steady laminar flow of Newtonian fluid. Continuity and Navier-Stokes equations in axial and radial directions are the governing equations that describe the flow and can be written as,

$$\frac{\partial u}{\partial x} + \frac{1}{r} \frac{\partial(rv)}{\partial r} = 0 \quad (1)$$

$$\frac{\partial(\rho uu)}{\partial x} + \frac{1}{r} \frac{\partial(\rho rvu)}{\partial r} = \frac{\partial}{\partial x} \left(\mu \frac{\partial u}{\partial x} \right) + \frac{1}{r} \frac{\partial}{\partial r} \left(\mu r \frac{\partial u}{\partial r} \right) - \left(\frac{\partial p}{\partial x} \right) \quad (2)$$

$$\frac{\partial(\rho uv)}{\partial x} + \frac{1}{r} \frac{\partial(\rho rvv)}{\partial r} = \frac{\partial}{\partial x} \left(\mu \frac{\partial v}{\partial x} \right) + \frac{1}{r} \frac{\partial}{\partial r} \left(\mu r \frac{\partial v}{\partial r} \right) - \left(\frac{\partial p}{\partial y} \right) - \left(\frac{\mu v}{r^2} \right) \quad (3)$$

where $\rho (=1.205 \text{ kg/m}^3)$ is the air density to 20°C , $\mu (=1.81 \times 10^{-5} \text{ Pa}\cdot\text{s})$ is the absolute viscosity, u and v are, respectively, the axial and radial velocity components and p is the pressure. Equations (1) to (3) can be expressed by a single equation for the generic ϕ variable as,

$$\frac{\partial(\rho u \phi)}{\partial x} + \frac{1}{r} \frac{\partial(\rho rv \phi)}{\partial r} = \frac{\partial}{\partial x} \left(\Gamma^\phi \frac{\partial \phi}{\partial x} \right) + \frac{1}{r} \frac{\partial}{\partial r} \left(\Gamma^\phi r \frac{\partial \phi}{\partial r} \right) + S^\phi \quad (4)$$

where ϕ takes on the unitary value for Eq. (1), and u and v for Eqs. (2) and (3), respectively; Γ^ϕ and S^ϕ are the diffusion coefficients and source terms, respectively.

Attention will now be devoted to the boundary conditions that should be applied to the governing equations. At the outflow boundary local parabolic flow condition is applied, that is, $\partial(rv)/\partial r = u = 0$. At $r = 0$ the condition is $v = \partial u/\partial r = 0$. At the solid walls the non-slip condition is imposed, $v = u = 0$. At the entrance of the feeding orifice the axial velocity is determined from the prescribed Reynolds number, $u = U = \mu Re/(\rho d)$, and a null radial component of the velocity is imposed.

For the integration of the general governing differential equation, Eq. (4), using the finite volume methodology, the solution domain is divided in small non-overlapping control volumes. Next the differential equations are integrated along each control volume yielding a set of algebraic equations. The continuity equation is then transformed in an equation for pressure using the SIMPLE algorithm (Patankar, 1980), and the algebraic equations are solved by a Gauss-Seidel iterative procedure. It should be noted that when Eq. 4 is integrated along the control volumes that intercept the solid walls, the ELAFINT methodology (Udaykumar *et al.*, 1996; Ye *et al.*, 1999) is employed to capture the actual shape of the solid-fluid interface. Further details of the numerical methodology including a full description of ELAFINT can be found in Mariani (2002, 2006).

3. SOLUTION METHODOLOGY

A finite volume discretization scheme was used here to solve the governing differential equations. According to this practice the solution domain is divided into small non-overlapping control volumes and the continuity and momentum differential equations are integrated over each control volume (Patankar, 1980; Versteeg and Malalasekera, 1995). The resulting system of algebraic equations is solved using a combination of Thomas algorithm and the Gauss-Seidel method (see Patankar, 1980). The Semi Implicit Method for Pressure Linked Equations (SIMPLE) was used through of discretized form of continuity equation transformed into an equation for pressure.

An accuracy of the numerical solution is in the interpolation scheme employed to evaluate the variables at the control volume faces. In this work the Power Law Differencing Scheme (PLDS) described in Patankar (1980), considered of first order accuracy for the interpolated values.

Due to the strong non-linearity of the equations, under relaxation coefficients were required. For the velocity components these coefficients were 0.1 and for pressure 0.2. Convergence was stopped when the maximum residual of the algebraic equations was less than 10^{-6} . All results to be presented were obtained with an average mesh consisted of a $\times b = 100 \times 240$ grid points (radial \times axial). All points were hand placed with higher concentration in the regions of steeper gradients. The final mesh adopted in performing the computations was chosen after several grid independence tests were carried out.

4. RESULTS AND DISCUSSIONS

Validation of the numerical solution including the ELAFINT methodology is performed comparing computational and experimental pressure profiles along the valve reed for a situation where the valve is inclined 5° with respect to the horizontal position, as depicted in Figure 3. The valve parameters for the situation in the Figs. 3-5 are presented in Tab. 1.

Table 1 – Characteristics of computational simulations.

D (m)	e [m]	D [m]	s_c	Re
0.0349	0.0145	0.1047	0.012	1000 2000
0.0349	0.0145	0.1047	0.02	1000 2000
0.0349	0.0145	0.1047	0.03	1600 2000

Figures 3-5 present numerical and experimental results for the dimensionless pressure profiles along the valve reed. The dimensionless pressure is defined as $p^* = 2p/(\rho U^2)$ and is presented as a function of three dimensionless distance between valve seat and valve reed ($s_c/d = 0.012$; 0.02 and 0.03), and two Reynolds numbers ($Re = 1000$ and 2000 for cases A and B and 1600 and 2000 for case C). The experimental results were obtained from an existing experimental setup which was employed in previous investigations (see for instance Ferreira *et al.*, 1989).

Overall a good agreement prevailed between computation and experiment, except at the stagnation region. The agreement for $s_c/d = 0.02$ tend to be better than that for $s_c/d = 0.012$, so as the agreement for $s_c/d = 0.03$ tend to be better than that for $s_c/d = 0.02$. It should be pointed due to small distance between the valve seat and reed, where very high gradients are encountered for both pressure and velocity fields in this region. Those gradients impose many difficulties in solving the differential equation as well as in performing accurate experiments. For a description of the experimental uncertainty and the pressure sensitivity to small changes in the diffuser geometry the interested reader is referred to Ferreira *et al.* (1989). According to Ferreira *et al.* (1989) it is most likely that the large deviation between experiment and computation observed in the flat region of Figs. 3-5 are due to experimental difficulties, specially considering that a mesh refinement did not improved the numerical results at this region.

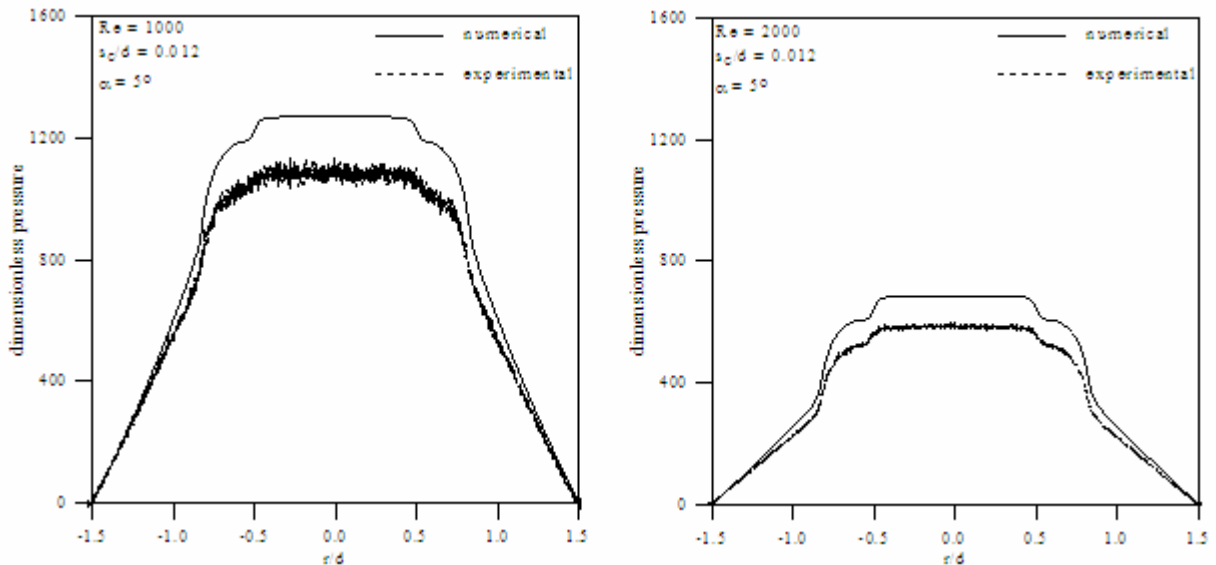


Figure 3. Numerical and experimental results for pressure distribution along valve reed for $Re = 1000$ and 2000 , $s_c/d = 0.012$ and $\alpha = 5^\circ$.

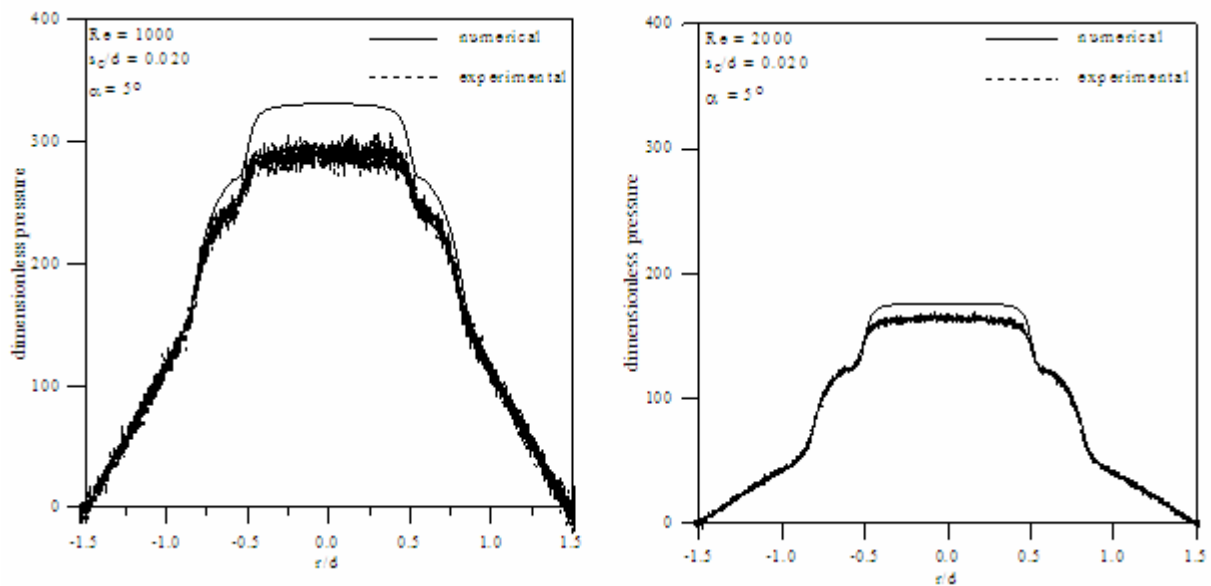


Figure 4. Numerical and experimental results for pressure distribution along valve reed for $Re = 1000$ and 2000 , $s_c/d = 0.02$ and $\alpha = 5^\circ$.

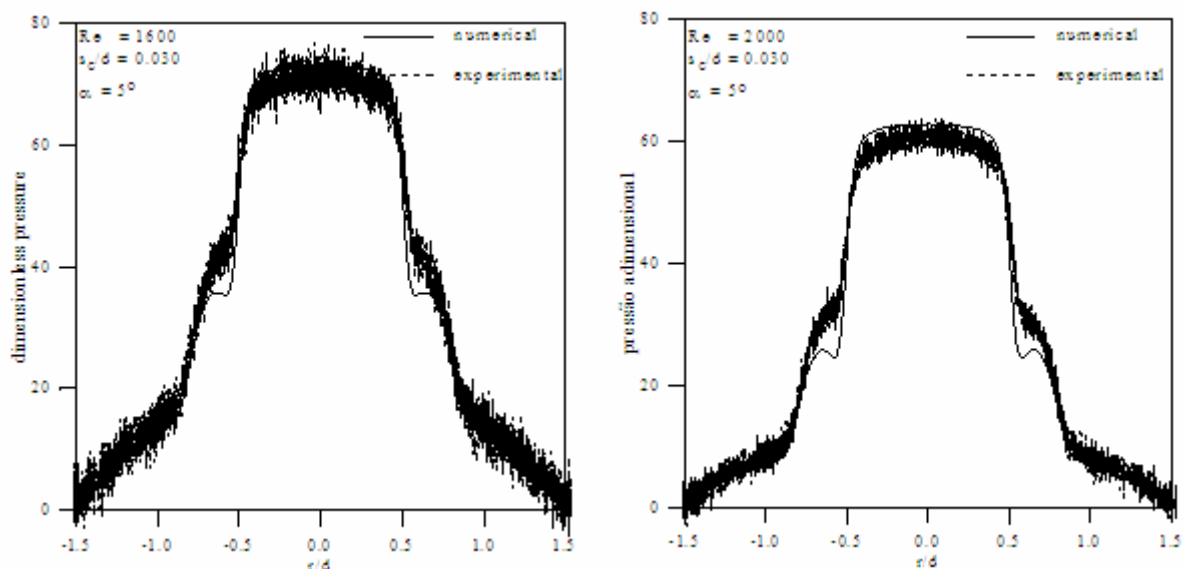


Figure 5. Numerical and experimental results for pressure distribution along valve reed for $Re = 1600$ and 2000 , $s_c/d = 0.03$ and $\alpha = 5^\circ$.

In Figs. 6 to 11 are presented numerical results for Reynolds numbers: 1000, 1500, 2000 and 2500 and inclinations seat: 0° , 5° and 32° .

The Figs. 6-8 shows that with the increase of the Reynolds number the pressure profiles along the valve reed decrease, because the fluid is accelerated with the increase of the velocity in the diffuser entrance and consequently it has a decreasing in the pressure levels. In these figures is perceived that with the gap increase between disks (reed and seat) tends to reduce pressure values. The use of an inclination of 5° in the seat (one chanfre in the diffuser entrance) makes with that the pressure levels have a significant decrease however modifying this inclination for approximately 30° does not perceive significant alterations.

As explored before, three parameters are very important in valve modeling and design: the force, the effective flow and force areas. Those parameters are generally used in numerical simulation of reciprocating hermetic compressors and can also be employed to evaluate the efficiency of the valves.

The effective flow area, A_{ee} , is directly related to the pressure drop through valve. For a given pressure drop A_{ee} can yield the mass flux through the valve. Thus, the higher the A_{ee} , the better is the performance of the valve with respect to the flow through it (Ussyk, 1984). The effective flow area is defined as

$$A_{ee} = \frac{\dot{m}}{p_u \sqrt{\frac{2k}{(k-1)RT_u}} \sqrt{r_p^{2/k} - r_p^{(k+1)/k}}} \quad (5)$$

where \dot{m} is the mass flow rate through the valve, $r_p = p_{atm}/p_u$, p_{atm} is the atmospheric pressure, p_u is the pressure upstream the valve, $k = c_p/c_v$, R is the gas constant, and T_u is the temperature upstream the valve. The dimensionless effective flow area is calculated by $A_{eea} = 4A_{ee}/\pi/d^2$.

The effective flow area is important in predicting the mass flow rate through the valve during suction and discharge. However, to calculate the valve movement it is necessary to know the force acting on the reed during each instant of time. This force is a result of the difference in pressure acting on both sides of the valve and depends on the flow and on the opening of the reed (Schwerzler and Hamilton, 1972). Usually the force on the valve is calculated through the effective force area, defined as,

$$A_{ef} = F/\Delta p_v \quad (6)$$

where Δp_v is the pressure difference through the valve.

The integration of the pressure distribution along the valve disc yielded the total force on the valve. The force is obtained by expression

$$F = 2\pi \int_0^{(D/2)} pr dr . \quad (7)$$

Results for the dimensionless force

$$F^* = \frac{2F}{\rho U_{in}^2 d^2} , \quad (8)$$

are given in Fig. 9 for two gap between disks studied in this work and for all Reynolds number.

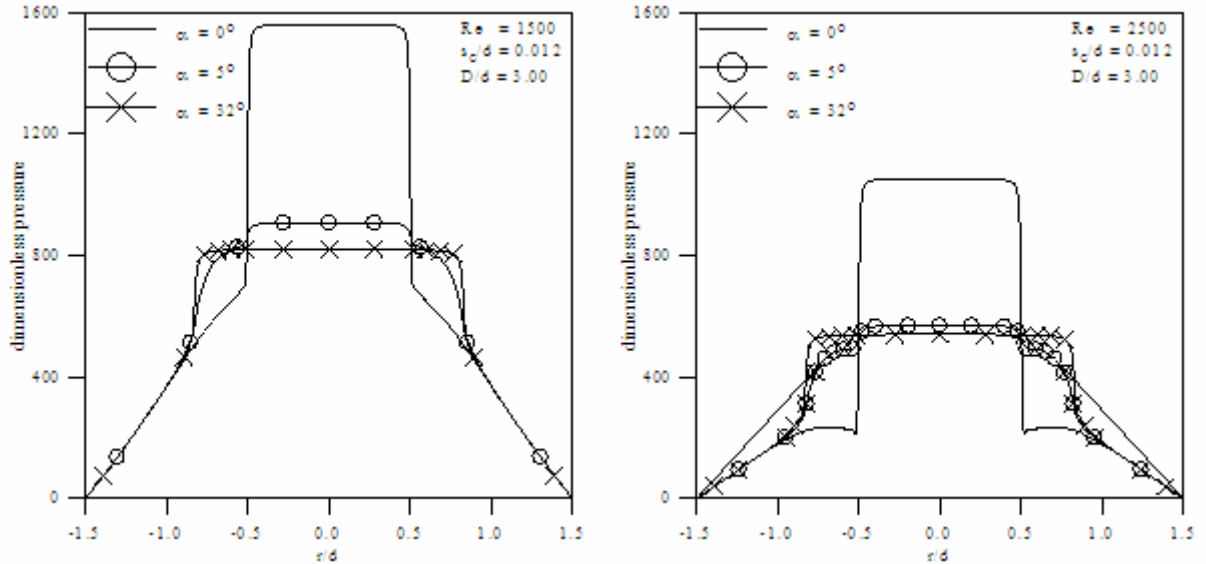


Figure 6. Numerical results for pressure distribution along valve reed for $Re = 1500$ and 2500 , $s_c/d = 0.012$, $\alpha = 0^\circ - 32^\circ$.

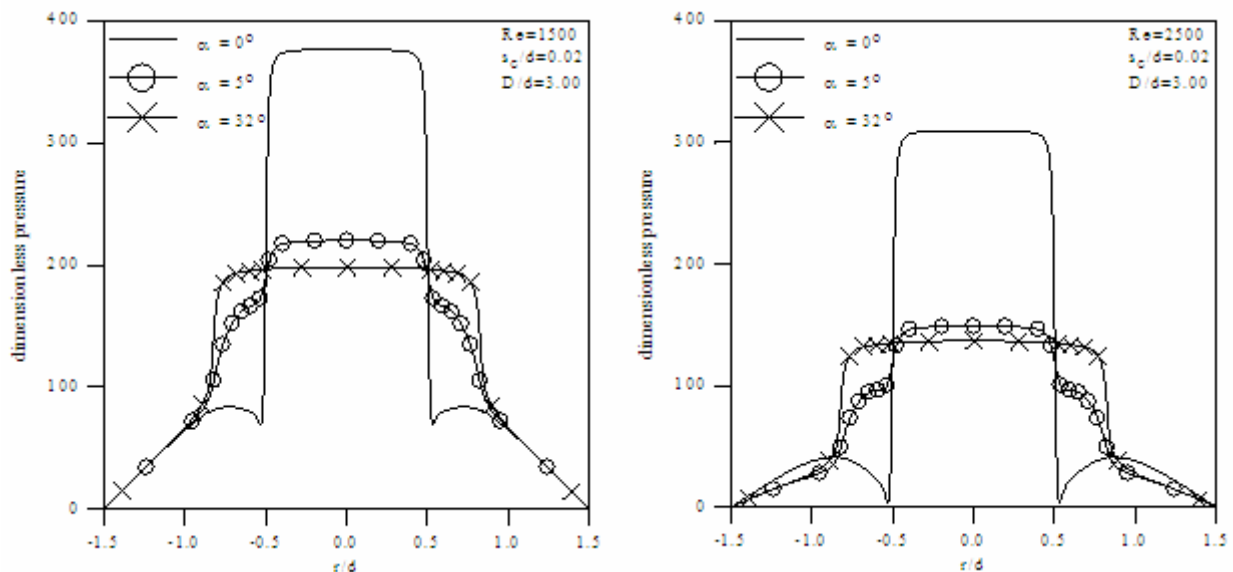


Figure 7. Numerical results for pressure distribution along valve reed for $Re = 1500$ and 2500 , $s_c/d = 0.02$, $\alpha = 0^\circ - 32^\circ$.

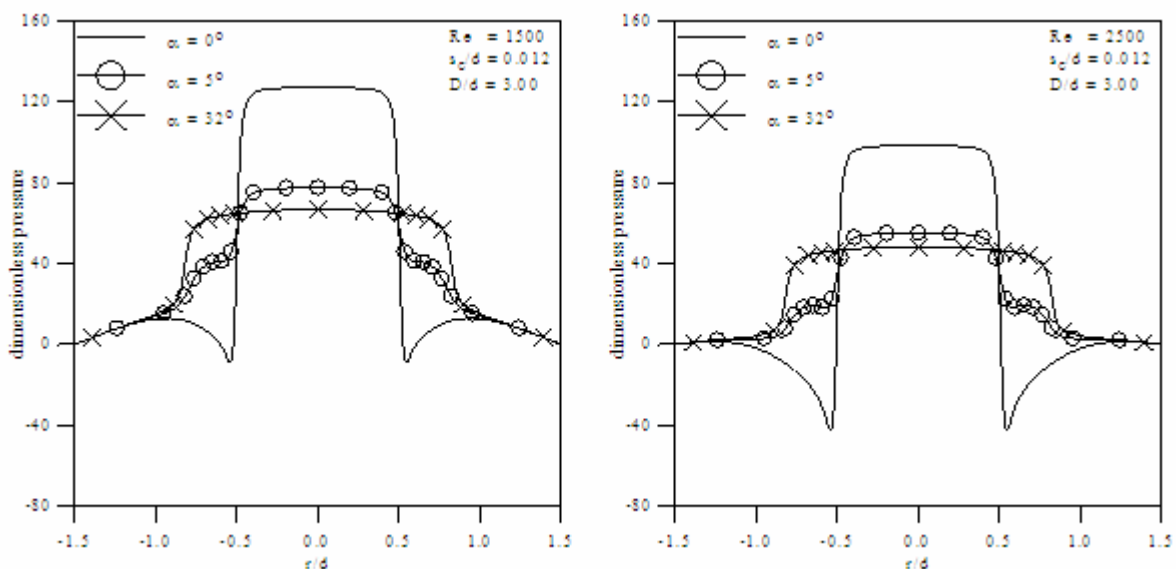


Figure 8. Numerical results for pressure distribution along valve reed for $Re = 1500$ and 2500 , $s_c/d = 0.03$, $\alpha = 0^\circ - 32^\circ$.

Figures 9 to 11 present numerical values of the dimensionless force, effective force and flow areas for $s_c/d = 0.012$ and 0.020 as a function of three inclinations on the radial diffuser having the Reynolds number as curve parameters.

Figure 9 presents the α influence on the dimensionless axial force. For the small values of s_c/d the force decreases as α increases because the stagnation pressure in the central region of the disc also diminishes. However, for certain combinations of Re and s_c/d (higher values) F increases with s_c/d . For those valve separation and flow rates the exit seat inclination tends to reduce the recirculating region in the flow field which is responsible for the presence of the negative pressure region on the valve disc.

Figure 10 show the variation of the dimensionless effective force area ($A_{efa} = 4A_{ef}/(\pi d^2)$) for $s_c/d = 0.012$ and 0.020 as a function of the geometry inclination modifications, for Reynolds numbers varying from 1000 to 2500. For both spacing between seat and reed, $s_c/d = 0.012$ and 0.020 , the dimensionless effective force area exhibits a monotonic behavior similar to that observed for the effective flow area, that is, as the modification parameter increases the effective force area increases. As seen in the figures, the use of inclination at the orifice outlet causes an increase in the effective force area that has a reduced impact for larger values of the inclination angle.

In general, the dimensionless effective flow area (A_{eea}) increases with the increasing value of the seat's inclination and of the Reynolds numbers. The presence of the seat inclination at the outlet of the feeding orifice provides a substantial increase in the dimensionless effective flow area, as observed in Figure 11. This result was also observed by

Puff *et al.* (1992), and can be explained noticing that the presence of the chamfer decelerates the fluid at the outlet of the feeding orifice which in turn increases the pressures by the Bernoulli effect. In Figure 11 it is observed that the use of the inclination results in expressive augmentations of the effective flow area when the angle changes from 0° to 5°. However, for inclinations larger than 5° little influence is observed in the A_{eff} value, especially for $s_0/d = 0.012$, no matter which Reynolds number is considered.

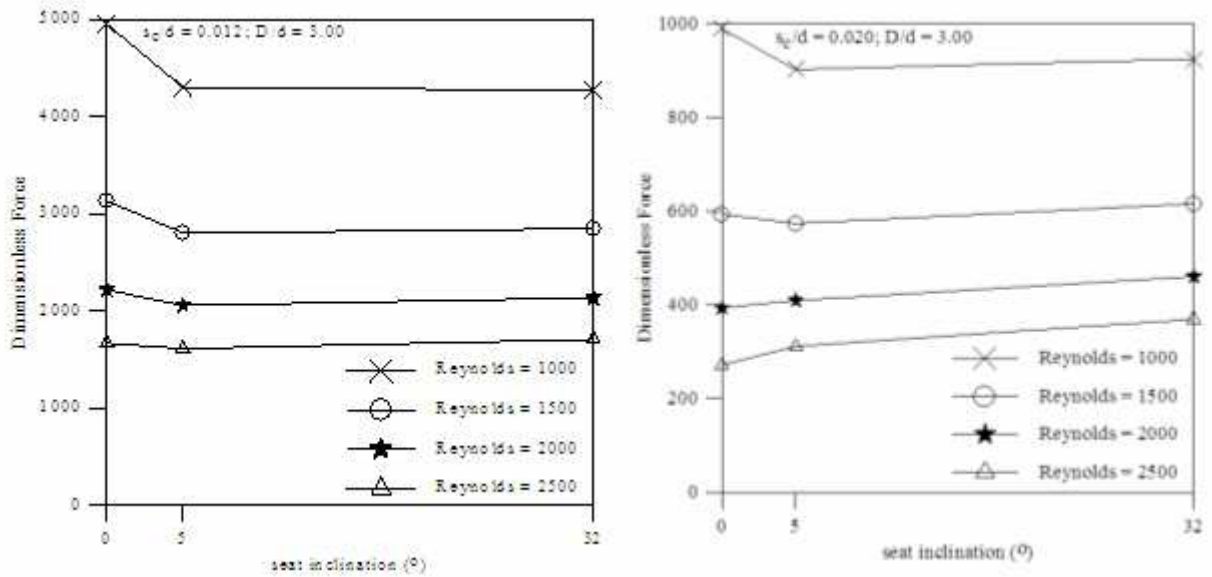


Figure 9. Influence of seat's inclinations on the dimensionless force.

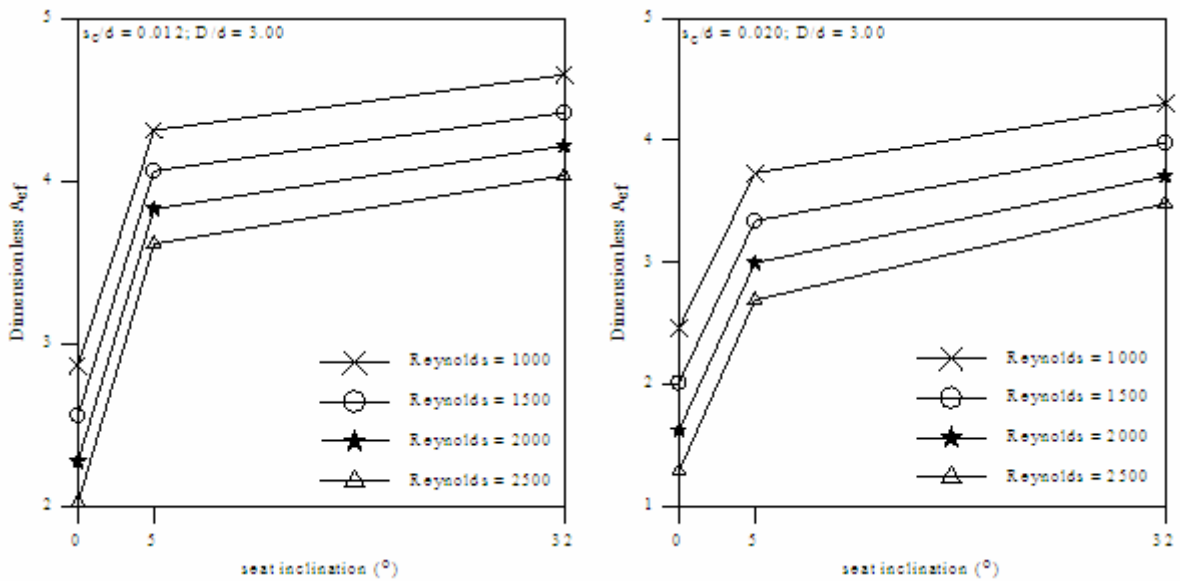


Figure 10. Influence of seat's inclinations on the dimensionless effective force area.

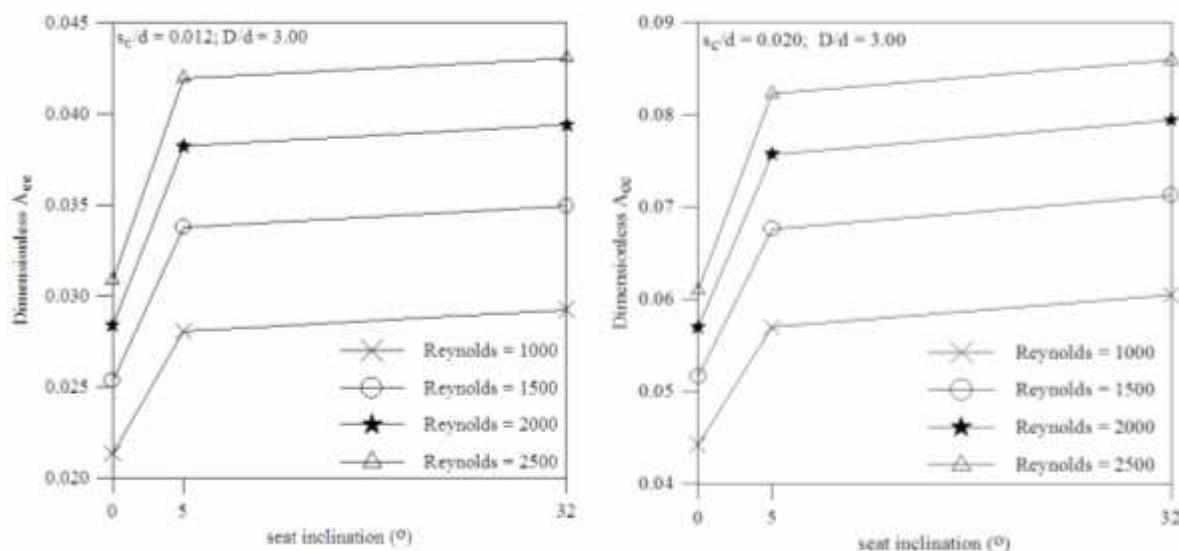


Figure 11. Influence of seat's inclinations on the dimensionless effective flow area.

5. CONCLUSIONS

The current work numerically investigated the flow in radial diffusers, such geometry approximates the geometry of automatic valves in reciprocating hermetic compressors which is the most common compressor employed in domestic refrigerators. Performance of those valves is entirely controlled by the flow itself, and for designing purposes it is convenient to express the mass flow rate through the valves and the force acting on their reed in terms of three parameters known as force, effective flow and force areas. The present work explored the impact that small seat's inclination changes of the valve have on the pressure, force, effective flow and force areas. The current analysis concluded that small modifications on the seat's inclinations valve geometry cause a significant increase in effective flow and force areas. For example, a seat inclination of only 5° is capable of altering the effective flow area by 30 % which is an expressive change.

6. ACKNOWLEDGEMENTS

The support of *Associação Paranaense de Cultura, APC*, in providing scholarships for the first and second authors is greatly appreciated. This work is part of a project under Grant 3-1-9130/2007 between Pontifical Catholic University of Parana and *Fundação Araucária*.

7. REFERENCES

- Deschamps, C. J., Prata, A. T. and Ferreira, R. T. S., 2000, "Modeling of turbulent flow through radial diffuser", *Journal of the Brazilian Society of Mechanical Sciences*, Vol. XXII, no. 1, pp. 31-41.
- Ervin, J. S. Suryanarayana, N. V. and Ng, H. C., 1989, "Radial, turbulent flow of a fluid between two coaxial disks", *ASME Journal Fluids Eng.*, Vol. 111, pp. 378-383.
- Ferreira, R. T. S. and Driessen, J. L., 1986, "Analysis of the influence of valve geometric parameters on the effective flow and force areas". In: *Ninth Purdue Compressors Technology Conference West Lafayette, USA*, pp. 632-646.
- Ferreira, R. T. S., Deschamps, C. J. and Prata, A. T., 1989, "Pressure distribution along valve reeds of hermetic compressors", *Experimental Thermal and Fluid Sciences*, Vol. 2, pp. 201-207.
- Hayashi, S., Matsui, T. and Ito, T., 1975, "Study of flow and thrust in nozzle-flapper valves", *ASME Journal Fluids Eng.*, Vol. 97, pp. 39-50.
- Mariani, V. C., 2002, "Methods of optimization and interface modeling techniques for analysis of fluid flow in radial diffuser with irregular geometries", Thesis (in portuguese), Department of Mechanical Engineering, Federal University of Santa Catarina, Brazil.
- Mariani, V. C. and Prata A. T., 2006, "Computational Modeling of Fluid Flow in Radial Diffusers With Irregular Boundaries", *Proceedings of 5th International Conference on Nuclear Engineering*, Chicago, USA.
- Matos, F. F. S., 2002, "Análise Numérica do Comportamento Dinâmico de Válvulas Tipo Palheta em Compressores Alternativos", Tese de Doutorado, Curso de Engenharia Mecânica, Universidade Federal de Santa Catarina, Brasil.
- Patankar, S. V., 1980, "Numerical Heat Transfer and Fluid Flow", McGraw-Hill.

- Possamai, F. C., Ferreira, R. T. S. and Prata, A. T., 2001, "Pressure distribution in laminar radial flow through inclined disks", *International Journal of Heat and Fluid Flow*, 22, pp. 440-449.
- Prata, A. T. and Ferreira, R. T. S., 1990, "Heat transfer and fluid flow considerations in automatic valves of reciprocating compressors", *Proceedings of the 1990 International Compressor Engineering Conference*, West Lafayette, USA, Vol. 1, pp. 512-521.
- Prata, A. T., Pilichi, C. D. M. and Ferreira, R. T. S., 1995, "Local heat transfer in axially feeding radial flow between parallel disks", *ASME Journal Heat Transfer*, Vol. 117, pp. 47-53.
- Puff, R., Prata, A. T. and Ferreira, T. S., 1992, "Effective flow and force areas for different geometries of compressor valves with laminar flow", *4th Brazilian Congress of Thermal Engineering and Sciences, ENCIT*, Rio de Janeiro, pp. 537-540.
- Salinas-Casanova, D. A., 2001, "Análise Numérica do Escoamento Turbulento em Válvulas Automáticas de Compressores", Tese de Doutorado, Curso de Engenharia Mecânica, Universidade Federal de Santa Catarina, Brasil.
- Schwerzler, D. D. and Hamilton, J. F., 1972, "An Analytical for Determining Effective Flow and Force Areas for Refrigeration Compressor Valving Systems", *International Compressor Engineering Conference at Purdue*, West Lafayette, Indiana, Vol. I, pp. 30-36.
- Tabatabai, M. and Pollard, A., 1987, "Turbulence in radial flow between parallel disks at medium and low Reynolds numbers", *Journal Fluid Mechanics*, Vol. 185, pp. 483-502.
- Udaykumar, H. S., Shyy, W. and Rao, M. M., 1996, "ELAFINT: A Mixed Eulerian-Lagrangian Method for Fluid Flows with Complex and Moving Boundaries", *International Journal for Numerical Methods in Fluids*, Vol. 22, pp. 691-712.
- Ussyk, M. S., 1984, "Simulação Numérica do Desempenho de Compressores Herméticos Alternativos", Dissertação de Mestrado. Departamento de Engenharia Mecânica, UFSC.
- Ye, T., Mittal R., Udaykumar, H. S. and Shyy, W., 1999, "An accurate cartesian grid method for viscous incompressible flows with complex immersed boundaries", *Journal of Computational Physics*, Vol. 156, pp.209-240.

8. RESPONSIBILITY NOTICE

The authors are the only responsible for the printed material included in this paper.